

Electronic Structure, Bonding, and Electrical Properties of  $\text{MoNiP}_8$ <sup>†</sup>Miquel Lluell,<sup>‡</sup> Santiago Alvarez,<sup>§</sup> and Pere Alemany<sup>\*,‡</sup>

Departament de Química Física and Departament de Química Inorgànica, Universitat de Barcelona, Diagonal 647, 08028 Barcelona, Spain

Roald Hoffmann

Department of Chemistry, Cornell University, Ithaca, New York 14853-1301

Received February 22, 1996<sup>⊗</sup>

Bonding in the recently synthesized transition metal pnictide  $\text{MoNiP}_8$ , which contains an unusual cubic coordination of Mo and unique  $\text{P}_8$  building blocks, has been analyzed by means of electronic band structure calculations using the semiempirical extended Hückel tight-binding method. Calculated densities of states suggest important covalent character for this compound, which is in good agreement with the experimentally observed electrical and magnetic properties. Departure from an ideal cubic structure for the  $\text{P}_8$  clusters present in this phase can be explained by the strong orbital mixing between these units and their environment in the solid.

Many phosphorus-rich transition-metal polyphosphides with  $\text{MP}_4$  stoichiometry are known.<sup>1–16</sup> They exhibit rich structural variation, crystallizing in 11 different structural types. In all these compounds, the phosphorus sublattice, formed by linking together puckered 10-membered rings, is usually described formally as  $\text{P}_4^{2-}$ , without necessarily implying the existence of four-membered rings. In these compounds the transition metal is coordinated octahedrally by six phosphorus atoms. The known structural types differ by (a) the way in which the  $\text{P}_{10}$  rings are condensed, (b) the way in which the coordination octahedra around the metal atoms are linked together, and (c) the existence or absence of metal–metal contacts to form either pairs or chains of metal atoms. A typical structure pertaining to this family of compounds is shown in Figure 1.

Ternary phases with a transition metal to phosphorus ratio of 1:4 are also known. In these compounds ( $\text{MoFe}_2\text{P}_{12}$ ,  $\text{WFe}_2\text{P}_{12}$ ,  $\text{TiMn}_2\text{P}_{12}$ ,  $\text{NbMn}_2\text{P}_{12}$ ,  $\text{WMn}_2\text{P}_{12}$ , and  $\text{MoMn}_2\text{P}_{12}$ )<sup>17–19</sup> the early transition metal has a square-antiprismatic coordination

while iron or manganese occupy octahedral positions. The anionic substructures found in these ternary phases differ from those found for the binary compounds:  $\text{MoFe}_2\text{P}_{12}$  and  $\text{WFe}_2\text{P}_{12}$  have one-dimensional chains of six-membered phosphorus rings, while complex three-dimensional nets with 18-membered phosphorus rings are found for  $\text{TiMn}_2\text{P}_{12}$  and the isotypical compounds  $\text{NbMn}_2\text{P}_{12}$ ,  $\text{MoMn}_2\text{P}_{12}$ , and  $\text{WMn}_2\text{P}_{12}$ .

Recently Dewalsky and Jeitschko<sup>20</sup> reported the synthesis of  $\text{MoNiP}_8$  and  $\text{WnP}_8$ , two ternary phosphides in which the early transition metal is coordinated by an almost perfect cube formed by eight phosphorus atoms, while nickel atoms occupy octahedral holes. In this case, the anionic substructure is formed by discrete  $\text{P}_8$  units that can be derived from a cube by breaking three of its 12 edges. The structure is shown in Figure 2.

Chemical bonding in all these phosphorus-rich phases has been discussed using the classical concept of two-electron bonds, where two electrons are assigned to each M–P or P–P short distance. In all these compounds each phosphorus atom has four closest neighbors (M or P) forming an approximately tetrahedral coordination environment. According to the octet rule, each P atom shares eight electrons with its nearest neighbors. Assuming that the two electrons of a M–P bond can be assigned to the phosphorus atom and that the two electrons of a P–P bond are assigned one to each phosphorus atom, we arrive at a formal oxidation number of 0 for the P atoms bound to one metal and three other phosphorus atoms. For those P atoms bonded to two metals and two phosphorus atoms the formal oxidation number is –1.

Following this reasonable electron-counting scheme, in the case of  $\text{MFe}_2\text{P}_{12}$  (M = Mo, W) Flörke and Jeitschko<sup>17</sup> give formal oxidation states of  $\text{M}^{4+}$  ( $d^2$ ) and  $\text{Fe}^{2+}$  ( $d^6$ ) for the transition metals. These authors ruled out alternative oxidation states (e.g.  $\text{Mo}^0/\text{Fe}^{4+}$  or  $\text{Mo}^{2+}/\text{Fe}^{3+}$ ) because they are not compatible with the diamagnetic behavior observed for these compounds. With these oxidation states one would expect a filled  $t_{2g}$ -type band for the iron atoms and an occupied nonbonding  $d_z^2$ -type band<sup>21</sup> for the Mo (W) atoms in a square-antiprismatic

<sup>†</sup> Dedicated to Prof. Wolfgang Jeitschko on his 60th birthday.

<sup>‡</sup> Departament de Química Física.

<sup>§</sup> Departament de Química Inorgànica.

<sup>⊗</sup> Abstract published in *Advance ACS Abstracts*, July 1, 1996.

- Hulliger, F. *Struct. Bonding* **1968**, 83.
- Jeitschko, W.; Ruehl, R.; Krieger, U.; Heiden, C. *Mater. Res. Bull.* **1980**, 15, 1755.
- Ruehl, R.; Jeitschko, W. *Acta Crystallogr., Sect. B* **1981**, 37, 39.
- Jeitschko, W.; Ruehl, R. *Acta Crystallogr., Sect. B* **1979**, 35, 1953.
- Ruehl, R.; Jeitschko, W.; Schwochau, K. *J. Solid State Chem.* **1982**, 44, 134.
- Krebs, H.; Mueller, K. H.; Zuern, G. Z. *Anorg. Allg. Chem.* **1956**, 285, 15.
- Jeitschko, W.; Donohue, P. C. *Acta Crystallogr., Sect. B* **1972**, 28, 1893.
- Evain, M.; Brec, R.; Fiechter, S.; Tributsch, H. *J. Solid State Chem.* **1987**, 71, 40.
- Sugitani, M.; Kinomura, N.; Koizumi, M.; Kume, S. *J. Solid State Chem.* **1978**, 26, 195.
- Jeitschko, W.; Braun, D. J. *Acta Crystallogr., Sect. B* **1978**, 34, 3196.
- Gibinski, T.; Cisowska, E.; Zdauwicz, W.; Henkie, Z.; Wojakowski, A. *Kristall. Tech.* **1974**, 9, 161.
- von Schnering, H. G.; Menje, G. Z. *Anorg. Allg. Chem.* **1976**, 422, 219.
- Nolaeng, B. I.; Tergenius, L. E. *Acta Chem. Scand., Ser. A* **1980**, 34, 311.
- Jeitschko, W.; Donohue, P. C. *Acta Crystallogr., Sect. B* **1975**, 31, 574.
- Braun, D. J.; Jeitschko, W. Z. *Anorg. Allg. Chem.* **1978**, 445.
- Jeitschko, W.; Floerke, U.; Scholz, U. D. *J. Solid State Chem.* **1984**, 52, 320.

(17) Flörke, U.; Jeitschko, W. *Inorg. Chem.* **1983**, 22, 1736.

(18) Scholz, U. D.; Jeitschko, W. Z. *Anorg. Allg. Chem.* **1986**, 540, 234.

(19) Scholz, U. D.; Jeitschko, W.; Reehuis, M. *J. Solid State Chem.* **1988**, 74, 260.

(20) Dewalsky, M. V.; Jeitschko, W. *Acta Chem. Scand.* **1991**, 45, 828.

(21) Burdett, J. K.; Hoffmann, R. *Inorg. Chem.* **1978**, 17, 2553.

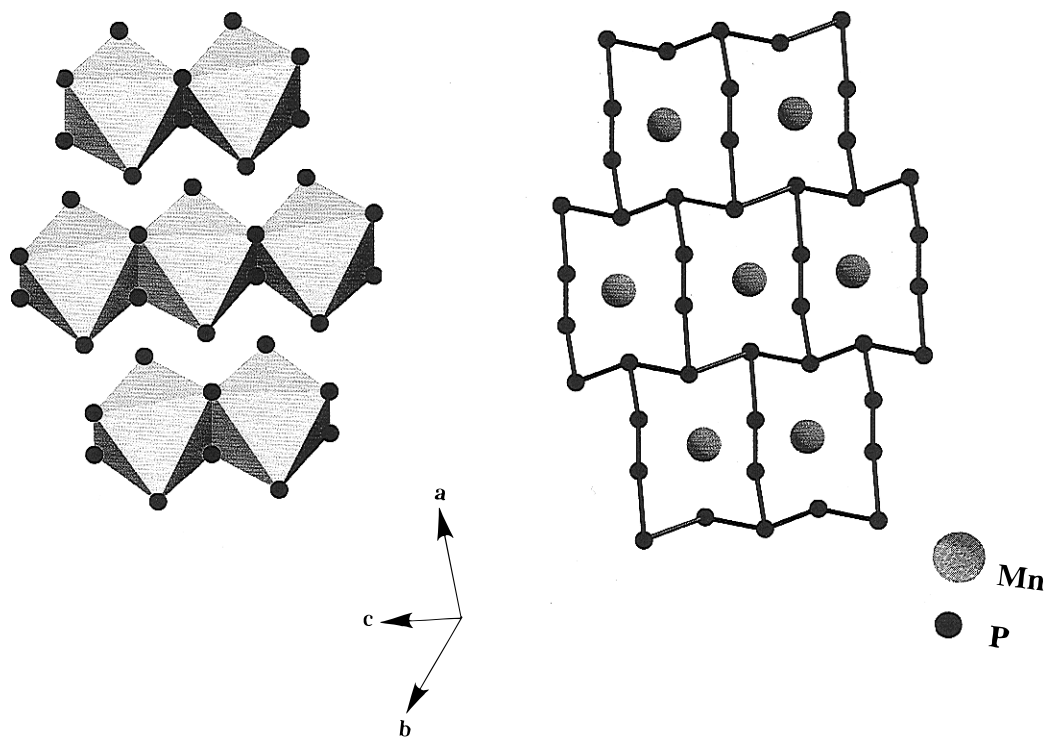


**Figure 1.** Representation of the crystal structure of  $2\text{-MnP}_4$  showing the coordination polyhedra around the metal atoms (a, left) and the phosphorus substructure (b, right).

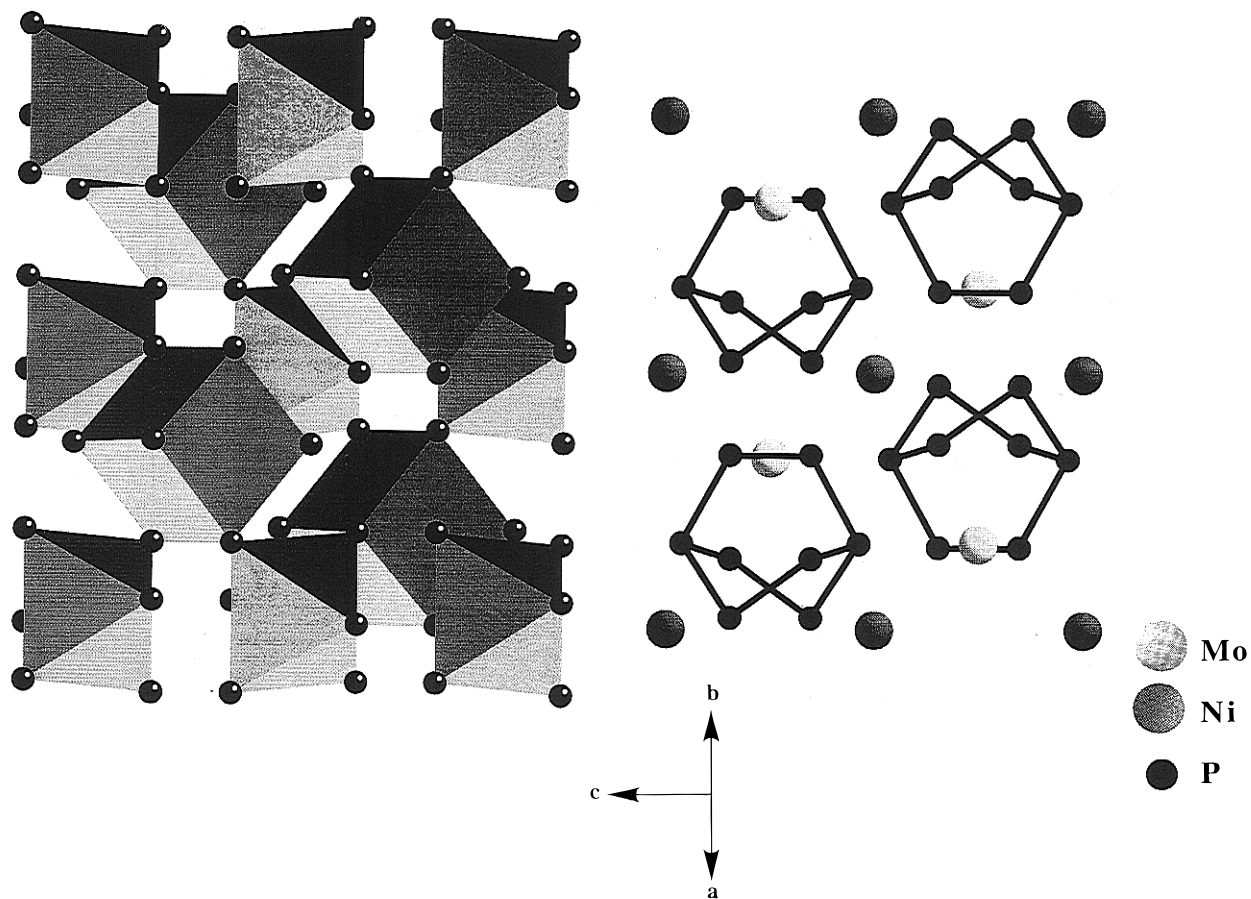


**Figure 2.** Representation of the crystal structure of  $\text{MoNi}_8$  showing the coordination polyhedra around the metal atoms (a, left) and the phosphorus substructure (b, right).

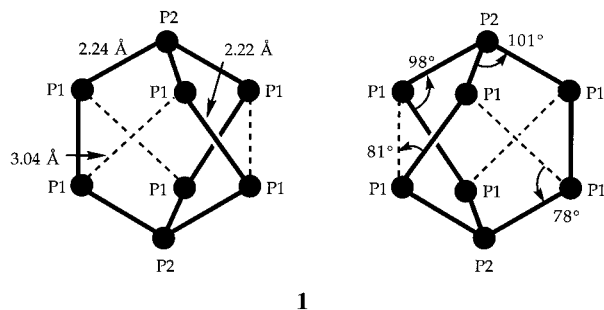
coordination environment. These oxidation states can indeed account for the semimetallic behavior of these compounds.

Bonding in  $\text{TiMn}_2\text{P}_{12}$  and in its isostructural compounds can also be rationalized by similar simple arguments. Formal oxidation states of  $\text{Ti}^{4+}[\text{Mn}^{4+}]_2[\text{P}_{12}]^{8-}$  have been proposed by Scholz

and Jeitschko.<sup>18</sup> In this case the nonbonding  $d_{22}$ -type band of the square antiprismatic units would be empty. The observed formation of Mn–Mn bonds in the  $\text{Mn}_2\text{P}_{10}$  units (edge-sharing octahedra) is in total agreement with the assignment of a  $\text{Mn}^{2+}$  ( $d^5$ ) oxidation state. The  $t_{2g}$  levels of both octahedra form six

combinations ( $\sigma$ ,  $\pi$ ,  $\delta$ ,  $\delta^*$ ,  $\pi^*$ , and  $\sigma^*$ ) from which only  $\sigma^*$  remains empty and a net single Mn–Mn bond is formed. The diamagnetic behavior of the compound is in good agreement with this electronic structure, although overlap between manganese-centered bands and other bands is necessary to account for the metallic conductivity measured for this compound.

Application of this simple bonding scheme to the new ternary phosphides, MoNiP<sub>8</sub> and WNiP<sub>8</sub>, has difficulties. Assignment of a  $-6$  charge,  $[\text{P}^-]_6[\text{P}^0]_2$ , to the discrete P<sub>8</sub> units with two three-coordinate and six two-coordinate P atoms, assuming three bonds broken in a cube (see **1**), leaves us with six positive



charges to be shared by both metal atoms. Dewalsky and Jeitschko<sup>20</sup> propose a formula with conventional oxidation numbers:  $\text{Mo}^{4+}\text{Ni}^{2+}[\text{P}_8]^{6-}$ . According to this electron count, two electrons would be accommodated in a Mo-centered, non-bonding band, while eight electrons would be occupying the nonbonding Ni  $t_{2g}$ -type band (six electrons) and the antibonding Ni  $e_g$ -type band (two electrons). With this formal oxidation state, the 18-electron rule, as usually applied, is not valid for the nickel atoms for which the formal count leads to 20 valence electrons per atom.

The metallic conductivity and Pauli paramagnetism found for these two new compounds would indicate the existence of a relatively broad Ni centered  $e_g$ -type band, which is in disagreement with the behavior observed for other  $\text{Ni}^{2+}$  compounds with octahedral coordination spheres: NiO, with a NaCl-type structure, is a typical Mott insulator in which the localized nature of the  $e_g$  levels leads to a much discussed failure of the band theoretical perspective.<sup>22–25</sup> Upon a decrease in the electronegativity of the main group element, a change in the electric properties is found:  $\text{NiX}_2$  ( $X = \text{Se}, \text{Te}$ ) with the pyrite structure<sup>26,27</sup> and  $\text{NiX}$  ( $X = \text{Se}, \text{Te}$ ) with the NiAs-type structure<sup>28,29</sup> are metallic conductors. In these cases, the partially filled  $e_g$ -type band probably has a large main group element contribution and is thus no longer strongly localized as in NiO. The properties of analogous sulfur compounds of nickel are found to lie somewhere between these two types of behavior:  $\text{NiS}_2$  with a pyrite structure<sup>26</sup> and  $\text{NiS}$  with the NiAs-type structure<sup>30</sup> are semiconductors, although they should be metallic according to their half-filled  $e_g$ -type bands.

In this work we will analyze in detail the electronic structure of MoNiP<sub>8</sub> using band structure calculations. Our main goal is to achieve a better understanding of the bonding relations in this complex structure and to attempt to correlate its observed

- (22) Fujimori, A.; Minami, F.; Sugano, S. *Phys. Rev. B* **1984**, *29*, 5225.  
 (23) Fujimori, A.; Minami, F. *Phys. Rev. B* **1984**, *30*, 957.  
 (24) Sawatzky, A.; Allen, J. W. *Phys. Rev. Lett.* **1984**, *53*, 2339.  
 (25) Zaanen, J.; Sawatzky, G. A.; Allen, J. W. *Phys. Rev. Lett.* **1985**, *55*, 418.  
 (26) Hulliger, F. *Helv. Phys. Acta* **1959**, *32*, 615.  
 (27) Bither, T. A.; Prewitt, C. T.; Gillson, J. L.; Bierstedt, P. E.; Flippen, R. B.; Young, H. S. *Solid State Commun.* **1966**, *4*, 533.  
 (28) Grønvdal, F.; Jacobsen, E. *Acta Chem. Scand.* **1956**, *10*, 1440.  
 (29) Matthias, B. T. *Phys. Rev.* **1953**, *92*, 874.  
 (30) Sparks, J. T.; Komoto, T. *Phys. Lett.* **1967**, *25A*, 398.

**Table 1.** Experimentally Determined Atomic Positions for MoNiP<sub>8</sub>

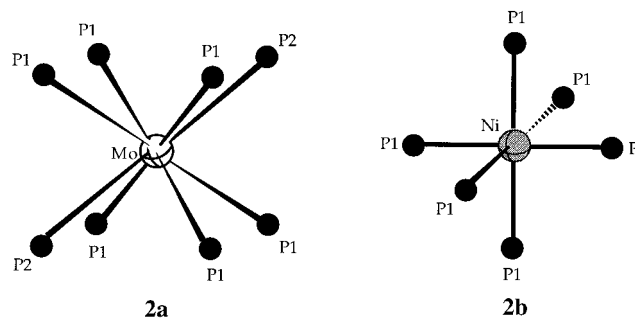
atom		x	y	z
Mo	2d	$\frac{2}{3}$	$\frac{1}{3}$	$\frac{1}{4}$
Ni	2b	0	0	0
P1	12i	0.046	0.321	0.153
P2	4f	$\frac{1}{3}$	$\frac{2}{3}$	0.037

electric and magnetic properties with the calculated electronic structure.

### Crystal Structure of MoNiP<sub>8</sub>

The nature of the highest occupied bands, responsible for the electronic properties of a material, is strongly dependent on both its composition and its crystal structure. A detailed knowledge of the geometrical features is thus crucial in analyzing the details of the electronic structure of a crystal. MoNiP<sub>8</sub> crystallizes in the  $P\bar{3}1c$  (No. 163) space group, with lattice parameters  $a = 6.235 \text{ \AA}$  and  $c = 8.747 \text{ \AA}$ .<sup>20</sup> The crystal structure has only four distinct atomic positions (see Table 1) and is therefore relatively simple if compared to the other ternary phosphide structures with a metal to phosphorus ratio of 1:4.

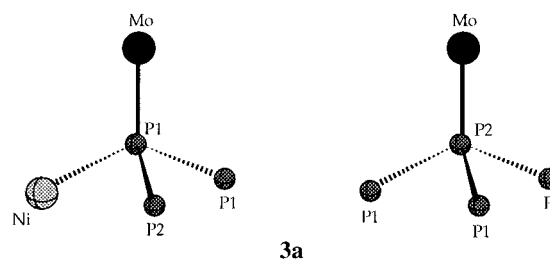
In this structure, as mentioned above, Mo atoms have eight phosphorus atoms forming an almost perfect cube as nearest neighbors (**2a**). This is, to our knowledge, the first transition-



metal phosphide with this type of coordination that has been described in the literature. A coordination number of 8 is also found for Mo atoms in  $\text{MoFe}_2\text{P}_{12}$ , although with a square-antiprismatic geometry.<sup>17</sup> The phosphorus cube around Mo has a small trigonal-antiprismatic distortion that makes the Mo–P distances slightly different: Mo–P1 = 2.54 Å and Mo–P2 = 2.51 Å, respectively.

The coordination sphere of Ni is formed by six phosphorus atoms in an octahedral geometry (Ni–P = 2.31 Å) with a small trigonal-antiprismatic distortion (**2b**). Similar coordination environments are found for nickel in other polyphosphides such as  $\text{NiP}_3$ <sup>31</sup> or in a high-pressure structure of  $\text{NiP}_2$ .<sup>32</sup>

The two different types of phosphorus atoms present in MoNiP<sub>8</sub> have the distorted tetrahedral environments shown in **3** formed by either two metals and two phosphorus atoms or



- (31) Rundqvist, S.; Ersson, N.-O. *Ark. Kemi* **1968**, *30*, 103.  
 (32) Donohue, P. C.; Bither, T. A.; Young, H. S. *Inorg. Chem.* **1968**, *7*, 998.

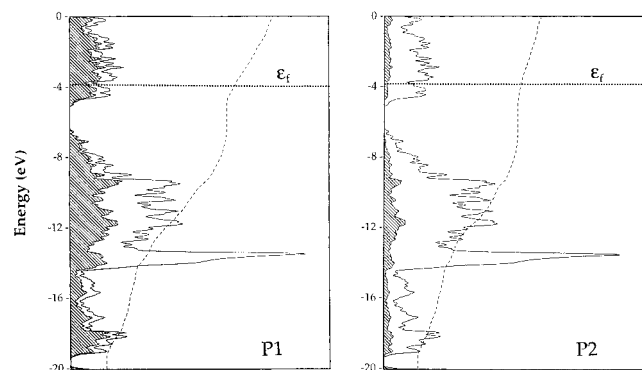


**Figure 3.** DOS curves for  $\text{MoNi}_8$ . The shaded areas correspond to the contributions of the P1 atoms (a, left) and P2 atoms (b, right) to the total DOS. The dashed curves correspond to the integrated DOS for the projected contributions.

one metal and three phosphorus atoms, similar to those found in many transition-metal polyphosphides.

The most interesting structural feature of  $\text{MoNi}_8$  is the phosphorus substructure, formed by two discrete, enantiomeric  $\text{P}_8$  units (see **1** and Figure 2b) per unit cell. These can be derived from a regular  $\text{P}_8$  cube by breaking three of its 12 edges, while maintaining one of the three  $C_3$  axes that run along the diagonals of the cube.

The crystal structure of  $\text{MoNi}_8$  is obtained from a complex stacking of vertex-sharing octahedra and cubes in all three dimensions (see Figure 2). Each nickel-centered octahedron shares its six vertices with six neighboring molybdenum-centered cubes, while each of these cubes is connected via common vertices to six neighboring octahedra. Two opposite vertices of each cube (those with P2 type phosphorus atoms) remain unlinked to other coordination polyhedra. The highly three-dimensional character of this structure does not allow us to describe it using simpler low-dimensional building blocks, except for the zero-dimension  $\text{P}_8$  units.

### Electronic Structure and Bonding of $\text{MoNi}_8$

Application of simple electron-counting rules to a material with a large degree of structural complexity often leads to an oversimplified picture that is only able to explain the rough features of bonding and its relation to the electric and magnetic properties of crystals. In order to gain a deeper understanding of the electronic structure of  $\text{MoNi}_8$  and its relation with the physical properties of this material, we performed tight-binding band structure calculations using the semiempirical extended Hückel method. The parameters used in this work together with other computational details are reported in the Appendix.

The density of states (DOS) curves in Figure 3 show that the metallic behavior of  $\text{MoNi}_8$  is correctly rationalized by our band calculations and that the highest occupied band is separated from the rest of occupied bands by a gap of approximately 1 eV. The phosphorus contribution is spread over the whole energy spectrum: all the bands below  $-14.5$  eV are built basically from the 3s atomic orbitals, while the contribution of 3p orbitals (especially on P1 atoms) is dominant in the regions around the Fermi level, indicating that the electric properties in this compound are probably associated with the phosphorus substructure.

### An "Inverse" Ligand Field Splitting

The d orbitals of a transition-metal atom in an octahedral or cubic environment show the well-known splitting into  $t_{2g}$  and  $e_g$  sets (**4**). These splitting patterns arise from the destabilization

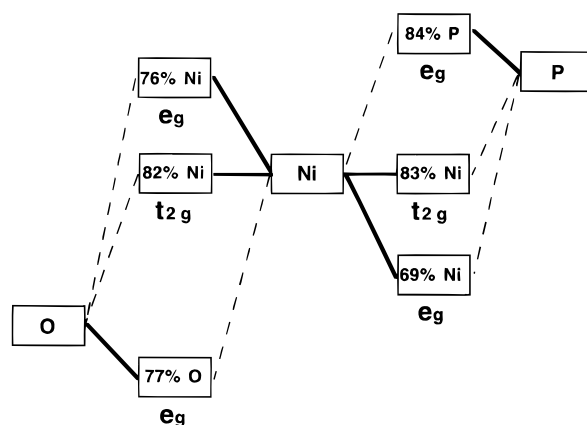
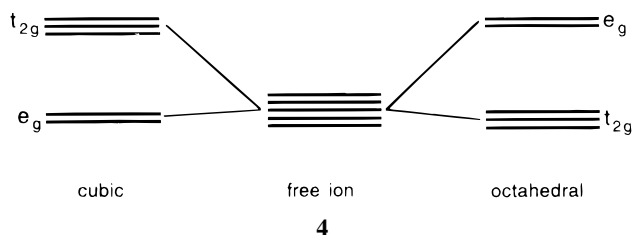


**Figure 4.** Schematic representation of the interaction of the metal d orbitals with an octahedral coordination sphere of strongly electronegative (left) or less electronegative (right) ligands. The main character of the resulting molecular orbitals, obtained from EH calculations on model octahedral  $\text{ML}_6$  compounds, is indicated for each case.

of some of the metal d orbitals due to their antibonding combination with ligand-centered  $\sigma$ -donor orbitals of the right symmetry, while other d orbitals remain at the same energy, essentially as metal-centered nonbonding orbitals. If the ligand



electronegativity is decreased, a more covalent picture of metal–ligand bonds has to be applied. The main difference is that in this case the splitting arises from the stabilization of some of the metal d orbitals due to the bonding combination with ligand-centered  $\sigma$ -donor orbitals of the right symmetry. This situation leads to an apparent “inverse” ligand field splitting of the d orbitals of the transition-metal atom as shown in Figure 4 for the octahedral case. The most important consequence is that in the case of strongly electronegative ligands one obtains metal-centered frontier orbitals, while in the case of less electronegative ligands the main contribution to the frontier orbitals is gradually shifted to the ligands.

Contributions of the d orbitals of Ni and Mo to the total DOS (Figure 5) appear in the middle region of the valence band, between  $-14$  and  $-9$  eV. No clear d orbital splitting can be observed for either of the two metals, partly due to the level broadening caused by the extended nature of the system. From Figure 5 it is also clear that in this compound the region around the Fermi level is formed basically by phosphorus-centered bands. In agreement with the “inverse” orbital splitting picture, the highest occupied band in  $\text{MoNi}_8$  is mainly built from phosphorus-centered orbitals of  $e_g$  symmetry around the nickel atoms and  $t_{2g}$  symmetry around the molybdenum atoms as can be deduced from the slight mixture of metal d orbitals of these symmetries in this region of the DOS.

A detailed analysis with help of the crystal orbital overlap population (COOP) curves (Figure 6) shows that, for both the nickel and the molybdenum atoms, all the metal-centered crystal orbitals are metal–ligand bonding in nature, consistent with an “inverse” splitting situation. The COOP curves reveal also the metal–ligand antibonding character of the orbitals close to the Fermi energy. A similar situation has also been found for the

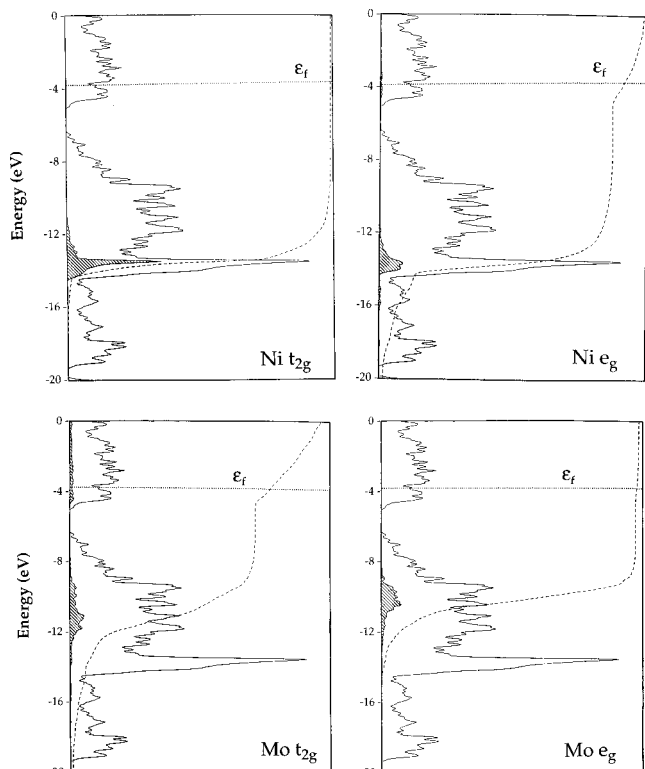


**Figure 5.** Transition metal d-orbital contributions to the DOS of MoNiP<sub>8</sub>. The shaded areas correspond to the contribution of the  $t_{2g}$ -type orbitals of nickel (a, top left),  $e_g$ -type orbitals of nickel (b, top right),  $t_{2g}$ -type orbitals of molybdenum (c, bottom left), and  $e_g$ -type orbitals of molybdenum (d, bottom right). The dashed curves correspond to the integrated DOS for the projected contributions.

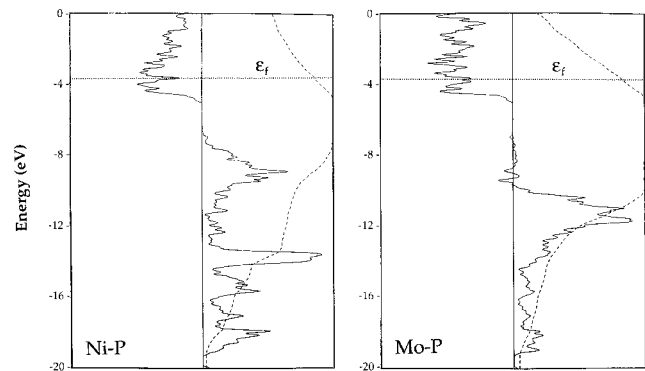


**Figure 6.** COOP curves for the Ni–P bonds (a, left) and Mo–P bonds (b, right). The dashed curves correspond to the integration of the COOP.

skutterudite-type NiP<sub>3</sub> and CoP<sub>3</sub> polyphosphides.<sup>33</sup> For these two compounds, ab-initio band structure calculations of the LMTO–ASA type confirm the “inverse” splitting scheme at the metal d orbitals coordinated by six P atoms in an octahedral fashion.

Are there any interesting consequences arising from this “inverse” ligand field splitting situation found in MoNiP<sub>8</sub>? Yes, there are, both in the bonding nature of the compound and in its electrical properties. The “inverse” splitting situation invalidates the application for this compound of the simple electron-counting rules that lead to formal charges like Mo<sup>4+</sup>Ni<sup>2+</sup>[P<sub>8</sub>]<sup>6-</sup>, since such rules assume that electrons flow from the metal atoms to the phosphorus substructure due to the more electronegative character of the latter. Population analysis

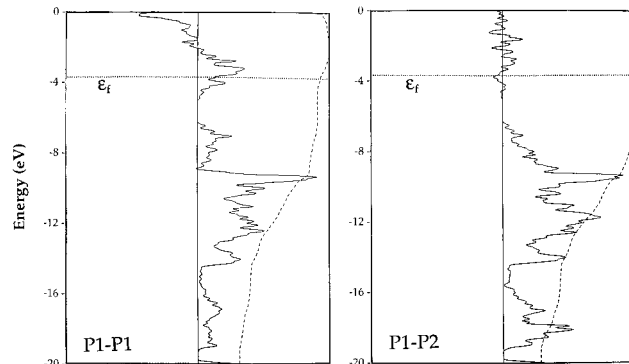


**Figure 7.** COOP curves for the P1–P1 bonds (a, left) and P1–P2 bonds (b, right). The dashed curves correspond to the integration of the COOP.

gives slightly positive charges for phosphorus atoms, while important electron filling of the d bands is found for both metals. These results, which are practically insensitive to the choice of the valence state ionization energies ( $H_{ii}$ 's) chosen for phosphorus, show that bonding in compounds like MoNiP<sub>8</sub> is essentially covalent in nature.

The Fermi level comes in a region of states which are almost entirely centered on the phosphorus atoms. The highest occupied band has an important contribution from all P atoms in the crystal and exhibits a considerable width, indicating thus a highly delocalized nature. This finding is in good agreement with the metallic conductivity and the Pauli type paramagnetism observed for MoNiP<sub>8</sub>. In general, for the transition metal phosphides one would not expect to find a metal to insulator transition similar to that observed for NiO. In this oxide, the strong electronegative character of the oxygen atoms leads to partially filled, metal-centered  $e_g$ -type orbitals with a small spatial extent, and these give strongly localized levels in the solid state. In contrast, the less electronegative character of phosphorus atoms results in mostly phosphorus-centered, strongly delocalized orbitals that give rise to a relatively broad band in the solid state. A broad, phosphorus-centered highest occupied band similar to that found for MoNiP<sub>8</sub> has also been obtained for NiP<sub>3</sub>, both at the LMTO–ASA and extended Hückel levels of theory.<sup>33</sup> To confirm this point, we would suggest a careful examination of the electronic structure of some late transition metal phosphides like NiP<sub>3</sub> or MoNiP<sub>8</sub> using X-ray and UV photoelectron spectroscopies.

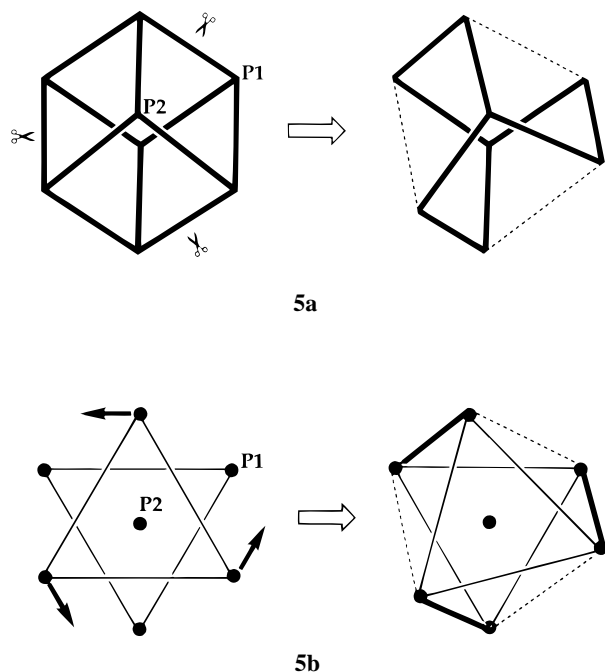
The phosphorus-centered nature of the crystal orbitals in the region around the Fermi level in MoNiP<sub>8</sub> also provides an explanation for the apparent violation of the 18-electron rule in this compound. The integrated COOP curves in Figure 6 show that filling the bottom of these bands up to the Fermi level results in a small decrease of both the Ni–P and Mo–P overlap populations. This loss in bonding is compensated by the P1–P1 bonding nature of the levels near the Fermi level, as shown in the COOP curves of Figure 7. The 18-electron rule is based on the assumption that filling the strongly metal–ligand antibonding  $e_g$  levels in an octahedral coordination compound will result in an unstable situation. In our case, the antibonding  $e_g$  levels are mostly ligand centered and their relatively small M–P antibonding character is largely compensated by the bonding character of these orbitals with those on P atoms belonging to neighboring coordination polyhedra. The Ni–P distance found in MoNiP<sub>8</sub> ( $d = 2.31 \text{ \AA}$ ) is relatively long when compared with those in other nickel phosphides (2.16–2.36  $\text{\AA}$ ). This finding is in good agreement with the occupation of the antibonding levels predicted in our calculations. The small variation of Ni–P distances in all known nickel-containing

(33) Lluell, M.; Alemany, P.; Alvarez, S.; Zhukov, V. P.; Vernes, A. *Phys. Rev. B* **1996**, *53*, 10605.

phosphides agrees however with the relatively small Ni–P antibonding character found for these bands.

### Shape of the $P_8$ Units in $MoNiP_8$

The last structural aspect we wish to address in this work is related to the distortion that is found for the  $P_8$  units in the title compound. As we have mentioned earlier, starting with a perfect cube formed by eight phosphorus atoms, one has to break three of its 12 edges while maintaining one of the three  $C_3$ -axes that run along the diagonals of the cube to obtain the actual geometry of the  $P_8$  clusters in  $MoNiP_8$  (**5a**). An alternative



way to look at the structure of the  $P_8$  clusters, which is more useful for our purposes, is to describe them as trigonal antiprisms, formed by six P1 atoms, with two parallel triangular faces of the antiprism capped by P2 atoms (**5b**). The actual shape of the  $P_8$  units in  $MoNiP_8$  can be obtained by the rotation of one of these triangular faces around the axis passing through the two capping atoms, breaking in this way three P1–P1 bonds.

If we center our attention on the orbitals of a cubic cluster formed by eight main group element atoms, we will find that, by using the four  $sp^3$  hybrid orbitals of each atom, we can form a total of 32 orbitals for the cluster. Twelve of these orbitals have bonding character (the  $\sigma$  bonds along the 12 edges of the cube), eight remain nonbonding (out-pointing lone pairs), and the remaining 12 are antibonding combinations ( $\sigma^*$  levels). For neutral  $P_8$  units, we obtain a perfect cube with 12 P–P bonds and a lone pair on each vertex. If we consider the  $-6$  formal charge suggested by the simple electron-counting rules for these clusters in  $MoNiP_8$ , three extra orbitals will be filled. These are per force P–P antibonding, resulting in the breaking of three bonds, as found for the experimental structure. Our band structure calculations show that bonding in this compound is substantially covalent, with almost neutral phosphorus atoms. The problem that arises with this picture is to explain the observed distortion: How can we break three bonds while maintaining an overall neutral charge on the cluster?

The answer to this question comes from careful examination of the interactions of the  $P_8$  units with their environment in the complete crystal structure. For this purpose, we carried out band structure calculations for an idealized  $MoNiP_8$  structure containing  $P_8$  clusters with a regular bicapped-antiprismatic geometry

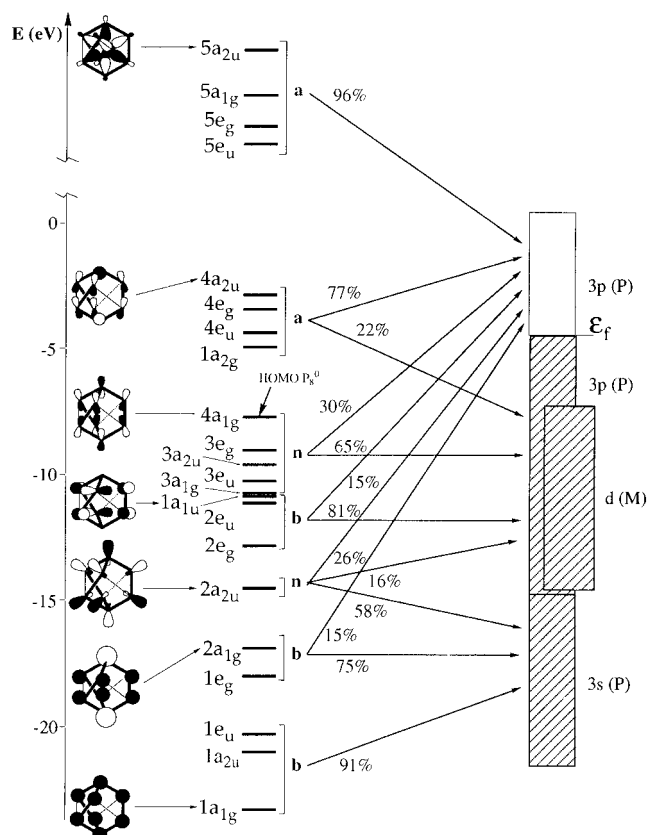


**Figure 8.** Schematic representation of the contribution of the molecular orbitals of a  $P_8$  cluster to the density of states of  $MoNiP_8$  (idealized structure). Percentages indicate the participation of each orbital set in the different regions of the density of states in the crystal. The symbols “b”, “n”, and “a” indicate the P–P bonding, nonbonding, and antibonding character of the cluster orbitals, respectively.

with 12 short P–P distances (P2–P1 = 2.31 Å, P1–P1 = 2.68 Å). We have not used a structure with perfectly cubic  $P_8$  units because in this case the structural rearrangement leads to a hypothetical crystal structure that is considerably different from the original one.

Figure 8 shows a comparison of the 32 orbitals obtained for an isolated  $P_8$  cluster with a schematic representation of the density of states of the whole crystal. The relative contribution of the orbitals of the free cluster to the different regions of the DOS is indicated by the arrows. The most important point to note is that the electron occupation of the phosphorus framework is strongly affected by the covalent interactions (orbital mixing) with the surrounding metal atoms. Some of the bonding orbitals have important contributions to bands that lie above the Fermi level, while some of the antibonding levels contribute considerably to the filled bands. For neutral isolated clusters we would have an occupation of 100% for the bonding and nonbonding orbitals and of 0% for the antibonding ones. By interaction with the surroundings, these orbital fillings are changed. A detailed analysis shows that some bonding orbitals are partially emptied (i.e. participate to some degree in the empty bands in the solid), resulting in a net occupation that decreases from 100% to 88%. The nonbonding orbitals, totally occupied in the isolated cluster, have only an average 72% occupation in the solid, while the antibonding  $\sigma^*$  levels increase their occupation from 0% to 14%.

The most significant change is for the nonbonding levels, primarily due to their orientation; they point “out” from the cluster, allowing a good overlap with the neighboring transition metal orbitals. The global balance is a 26% loss in bonding that corresponds almost exactly to the breaking of three P–P

bonds out of 12. This result indicates that orbital mixing alone is able to explain the distortion found for P<sub>8</sub> clusters in the real structure. Extrapolation of the electronic structure for the solid using isolated fragments can easily lead to wrong conclusions, especially in the case of strongly covalent compounds like MoNiP<sub>8</sub>.

### Concluding Remarks

The electronic structure calculations for MoNiP<sub>8</sub> reported in this paper, together with our earlier investigations on CoP<sub>3</sub> and NiP<sub>3</sub>, show that bonding in these compounds is essentially covalent in nature. Simple electron-counting rules are thus hardly applicable to these phases and can easily lead to wrong interpretations of the bonding relations. The strong covalent bonding affects the electric and magnetic properties of these materials: most of the late transition metal phosphides show metallic behavior in contrast to oxides and sulfides with similar coordination geometries that are semiconductors or insulators. Surprisingly, in the transition metal pnictides, the pnictide substructures rather than the metal atoms seem to be responsible for the observed electric and magnetic properties. A thorough spectroscopic study of the electronic structure for this vast family of compounds would indeed be of great value to clarify the complex bonding relations present in these interesting materials.

**Acknowledgment.** The stay of P.A. at Cornell University was made possible through a postdoctoral grant of the Ministerio de Educación y Ciencia of Spain. M.L. thanks the CIRIT (Generalitat de Catalunya) for a doctoral grant. The authors are grateful to E. Ruiz and E. Canadell for helpful comments on this work. Financial support of this work was provided by the DGICYT through Grant PB92-0655 and the CIRIT through Grant GRQ94-1077. Computing resources at the Centre de Supercomputació de Catalunya (CESCA) were generously made available by the Fundació Catalana per a la Recerca (FCR). The work at Cornell was supported by NSF Research Grant CHE 94-08455.

### Appendix

All band structure calculations presented in this work were obtained by using the extended Hückel tight-binding method.<sup>34–36</sup> The off-

**Table 2.** Atomic Parameters Used for the Extended Hückel Calculations on MoNiP<sub>8</sub>

atom	orbital	$H_{ii}$	$\zeta_{i1}$	$c_1$	$\zeta_{i2}$	$c_2$
P	3s	-18.40	1.81			
	3p	-9.80	1.45			
Mo	5s	-8.34	1.96			
	5p	-5.24	1.90			
	4d	-10.50	4.54	0.6097	1.90	0.6097
Ni	4s	-9.17	1.83			
	4p	-5.15	1.13			
	3d	-13.49	5.75	0.5683	2.00	0.6292

diagonal elements of the Hamiltonian matrix were evaluated with the modified Wolfsberg–Helmholz formula.<sup>37</sup> The atomic parameters used in this calculations are shown in Table 2. Parameters for P and Ni were taken from recent work on the electronic structure of skutterudite-type phosphides,<sup>33</sup> adjusting them to reproduce the DOS obtained for NiP<sub>3</sub> using the self-consistent LMTO–ASA method. The parameters used for Mo were proposed by Summerville and Hoffmann.<sup>38</sup> The  $H_{ii}$  values for the 3p orbitals of phosphorus adopted in our calculations deserve some further comment, since they differ clearly from those generally used in the EH method. Although the results presented in this work are practically insensitive to the choice of this parameter, a value of  $H_{ii}$  around of -10 eV seems to be more appropriate for p orbitals on phosphorus when its electronegativity is compared with that found for the rest of the elements close to P in the periodic table. Using the standard value of -14 eV for this parameter makes, for instance, P more electronegative than S, a situation that can result in a wrong description of the valence band region of compounds with both atom types in their composition.

Numerical integrations over the irreducible wedge of the Brillouin zone were performed using a 51K-point mesh obtained by the geometrical method of Ramírez and Böhm.<sup>39,40</sup>

IC9601955

(34) Hoffmann, R. *J. Chem. Phys.* **1963**, *39*, 1397.

(35) Whangbo, M.-H.; Hoffmann, R. *J. Am. Chem. Soc.* **1978**, *100*, 6093.

(36) Whangbo, M.-H.; Hoffmann, R.; Woodward, R. B. *Proc. R. Soc. London, A* **1979**, *366*, 23.

(37) Ammeter, J. H.; Bürgi, H. B.; Thibeault, J. C.; Hoffmann, R. *J. Am. Chem. Soc.* **1978**, *100*, 3686.

(38) Summerville, R. H.; Hoffmann, R. *J. Am. Chem. Soc.* **1976**, *98*, 7240.

(39) Ramírez, R.; Böhm, M. C. *Int. J. Quantum Chem.* **1986**, *30*, 391.

(40) Ramírez, R.; Böhm, M. C. *Int. J. Quantum Chem.* **1988**, *34*, 571.